Int. J. Adv. Res. Sci. Technol. Volume 13, Issue 09, 2024, pp.1521-1530.

IJARST

International Journal of Advanced Research in Science and Technology

https://doi.org/10.62226/ijarst2024132517

ISSN 2319 – 1783 (Print)

ISSN 2320 – 1126 (Online)

Modeling And Simulation of Rain Attenuation Effect on Microwave Propagation

[1*]F. U. Didigwu, [2]R. O. Okeke

[1, 2]Department of Electrical/Electronic Engineering, University of Port Harcourt, Nigeria.

[1]didigwu.fidelis@uniport.edu.ng, [2]remigius.okeke@uniport.edu.ng*

ARTICLEINFO

Article history:

Received	20 Sep 2024
Accepted	28 Sep 2024
Available online	08 Oct 2024

Keywords:

Rain Attenuation,
Frequency,
Excel software,
Python,
microwave propagation,
ITU-R models.

ABSTRACT

Rain attenuation poses a significant challenge to satellite communication networks, resulting in signal degradation, increased path loss, and reduced coverage, particularly in tropical regions and at frequencies above 10 GHz. This study examines average rain-induced attenuation and rainfall data for microwave links operating at 11 GHz, 13 GHz, 14 GHz, 18 GHz, and 23 GHz, with a rainfall rate of 50 mm/h, over a terrestrial link in Port Harcourt, Rivers State, Nigeria. The city's terrain, encompassing urban, suburban, and rural environments, serves as a representative model for broader applications across Nigeria. Situated in the coastal region, Port Harcourt experiences annual rainfall ranging from 2000 mm to 2400 mm. Satellite communication is frequently hindered by persistent rain attenuation, occasionally leading to outages lasting minutes, hours, or even days. Data for this analysis were sourced from the Nigerian Meteorological Agency (NIMET), and also the International Telecommunication Union's Radio-wave Propagation (ITU-R P.618-13) model was employed to estimate long-term rain attenuation for these frequency bands. Python and Excel software were used for data analysis and simulation. The results obtained show that higher frequencies experience greater attenuation. As the frequency increases, the rain attenuation also increases significantly. At any given percentage, attenuation increases with frequency. At 0.001%, 23 GHz has the steepest curve due to its higher attenuation value of 57.63 dB. Lower frequencies have relatively flatter curves, representing reduced attenuation. This helps to clearly show the trend at very small percentages of time. Attenuation decreases rapidly as the percentage of time exceeds increases. Also, the analysis revealed significant attenuation from June to September, coinciding with the peak rainfall period in the region. This study underscores the substantial impact of rain fade on signal attenuation at higher frequencies in Port Harcourt. The findings provide critical insights for satellite communication engineers to optimize the planning and design of microwave links in the region throughout the year.

1. Introduction

The growing demand for high data rates and capacity, coupled with the limitations of previous wireless generations in meeting these needs, has driven extensive research and development of 5G/6G communication networks [1]. These advanced networks are designed to deliver multi-gigabit-per-second (Gbps) data rates, exceptionally low latency, and improved quality of service (QoS), supporting critical applications such as e-health in rural areas, inclusive education, and bridging the digital divide [2].

Millimeter wave (mmWave) communication, operating within the 30–300 GHz frequency range, has emerged as a key candidate for 5G/6G networks and beyond, addressing the scarcity of sub-6 GHz spectrum [3]. The mmWave band offers enhanced security for communication transmissions and the large bandwidth necessary for achieving higher data rates in fronthaul, backhaul, and short building-to-building links [4]. However, a significant challenge of mmWave signals lies in their limited propagation distance, as they are highly susceptible to attenuation caused by atmospheric phenomena such as rain, foliage, and atmospheric absorption [5].

This research primarily aims to evaluate the impact of rain attenuation on radio frequencies. Among various atmospheric factors, rain is the leading cause of signal attenuation in microwave and millimeter wave communication, due to absorption and scattering effects on terrestrial and satellite links. The attenuation effect becomes particularly pronounced when the operating frequency

exceeds 10 GHz, especially in tropical regions prone to heavy and thunderous rain with significant depths [6]. Estimating its impact on link design remains unpredictable and challenging.

2. Study Area

Port Harcourt was established by the British colonial administration in Nigeria between 1912 and 1914. Geographically, it is situated between latitudes 4° 44' 58.8" N and 4° 56' 4.6" N, and longitudes 6° 52' 7.2" E and 7° 7' 37.7" E. The city experiences a tropical humid climate characterized by long, heavy rainy seasons and brief dry seasons. It receives abundant sunshine, with temperatures ranging from 25°C to 28°C [7].

As of the 2006 Census conducted in Nigeria, the urban population of Port Harcourt was estimated at 1,382,592. Road construction in this region faces significant challenges due to its unique terrain. The city lies on a low-lying coastal plain, geologically part of the sedimentary formation of the recent Niger Delta, with an elevation of less than 15.24 meters. Drainage in the area is poor, influenced by numerous surface water bodies and heavy annual rainfall, ranging from 2000 mm to 2400 mm [8].

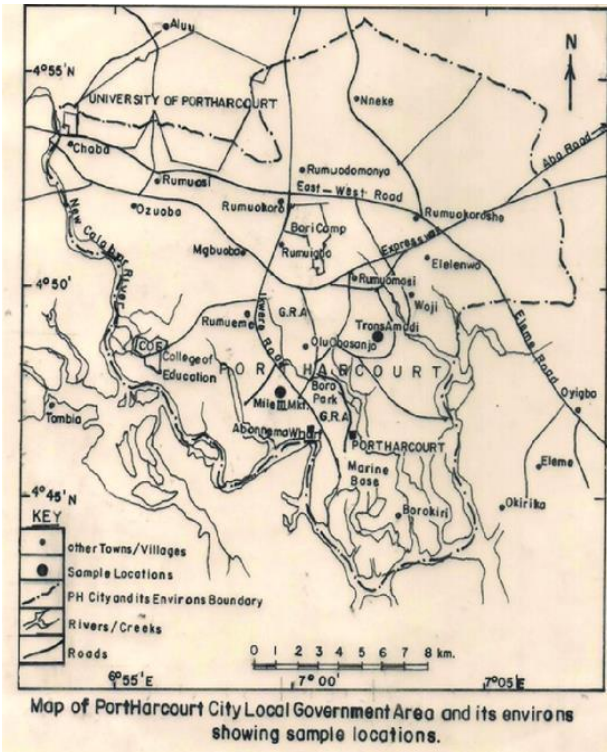

Map of PortHarcourt City Local Government Area and its environs showing sample locations.

Fig.1(a): Map of Port Harcourt City with different routes.

The coastal location of this city exposes it to frequent and intense rainfall, which has had a considerable impact on microwave communication systems. The persistent rainfall contributes to rain attenuation, a phenomenon where rain droplets absorb and scatter electromagnetic waves, weakening signal strength and degrading communication quality. This attenuation effect results in consistent signal distortions that can lead to communication outages lasting minutes, hours, or, in severe cases, even days. These disruptions have raised significant concerns among service providers, businesses, and researchers regarding the reliability of microwave communication networks. Addressing this challenge requires innovative strategies to mitigate the impact of rain attenuation. These could include employing robust fade mitigation techniques, optimizing link budgets with higher fade margins, leveraging alternative communication bands less affected by rain.

3. Literature Review

Numerous researchers and authors have made significant efforts to assess rain rate, rain attenuation, and signal degradation both within and outside Nigeria. For instance, [9] conducted a study using 1-minute rain rate data collected over two years in Akure, Nigeria. Measurements were obtained with an electronic weather station and a self-emptying tipping spoon, and the data was logged for analysis. The study employed validation techniques such as prediction error, RMSE, SC-RMSE, and Spearman's rank correlation. The findings revealed that no single model consistently provided a superior fit compared to others.

In Malaysia, research was conducted on the propagation of millimeter waves (mmWaves) over a 38 GHz link using real measurement data. The study utilized one year of rainfall data gathered over a 38 GHz line-of-sight link with a 300-meter path length and a sampling interval of 1 minute. Rain-induced attenuation distributions were evaluated against the modified ITU-R distance factor model at various time percentages to validate the model's accuracy. The results demonstrated excellent alignment between the modified model's predictions and the measured rainfall fade in Malaysia, as well as with data from other locations [10].

Additionally, the impact of rain attenuation on 5G networks was examined, and an optimal fade margin was proposed. Data was collected using a tipping bucket rain gauge and an RD-69 disdrometer, producing three separate datasets over different periods. The prediction model error, ε, was employed to validate the models, with its representation provided mathematically as:

$$\varepsilon_p = \frac{R_{est}(P) - R_{meas}(P)}{R_{meas}(P)} * 100\% \qquad 1$$

The findings indicated that the optimal attenuation margin for 5G should range from 6.5 to 10 dB for a 26 GHz link and 7 to 11 dB for a 28 GHz link [11]. In another study, [12] examined the effect of rain intensity on signal level measurements for millimeter-wave (mmWave) radio links over short distances, focusing on quantifying fading bias to achieve more accurate rain rate estimates. Measurements were conducted in line-of-sight scenarios using backhaul networks during rainy days in Beijing, China. These readings

were compared to local rainfall measurements obtained from a disdrometer and a rain gauge. At 25 GHz, wet testing revealed up to 4 dB loss caused by the water coating on the antenna. Even one hour after the rain had stopped, attenuation remained elevated due to residual moisture on the antenna. It was concluded that extended signal monitoring could quantify fading patterns more effectively.

Research by [13] investigated the impact of heavy rain on link performance to estimate attenuation accurately using dynamic rain fade measures for sustaining link connectivity. This study employed 17 years of rain data collected with two tools: the JW RD-80 disdrometer and a rain gauge, using three different sampling intervals. The study assessed which dynamic fade mitigation techniques were most suitable, utilizing a Backpropagation Neural Network (BPNN) to predict link conditions. The model was validated using rainfall events of varying intensities across multiple regimes, demonstrating that the BPNN outperformed other models in selecting effective rain fade mitigation strategies.

Another study examined signal attenuation above 60 GHz in Durban and Cape Town, South Africa. Measurements from two separate sites evaluated the specific attenuation coefficients relative to water droplet sizes at different temperatures as a function of frequency. The results revealed that specific attenuation increased with frequency, highlighting the influence of liquid water content (LWC) on signals [14].

A novel deep learning architecture was proposed by [15] to predict future rain fade using satellite and radar imagery data alongside link power measurements. Data from seven co-located sites for Echostar 19 and 24 were analyzed from Q4 2018 to Q1 2021. The model was compared with other machine learning approaches in terms of accuracy, precision, recall, and F1-score for both long- and short-term predictions. Results showed that the deep learning model outperformed its counterparts, particularly in long-term prediction accuracy.

Similarly, [16] employed a BPNN technique to predict rain attenuation using data from three terrestrial microwave links operating at 23 GHz and 38 GHz. The proposed model was validated using 38 GHz fade slope data and a chi-squared fitness test, demonstrating the model's efficiency for predicting rain attenuation in Nigeria. Another study used a machine learning-based adaptive spline model to predict rain attenuation across multiple frequencies and compared it to the power-law model. Data were obtained using a radiometer and a laser prediction monitor for frequencies ranging from 22.234 GHz to 30 GHz. Results showed that the adaptive spline model achieved greater accuracy than the power-law model, as measured by Minimum Mean Squared Error (MMSE) and Root Mean Square (RMS).

Finally, research in South Africa compared multiple models for real-time rain attenuation prediction for Earth-Space Communication Links (ESCL). Using 12 years of data from the South African Weather Service, the dataset was split for training and testing a proposed Artificial Neural Network (ANN). The ANN-based model was validated against existing models such as the ITU-R and Moupfouma models. Results indicated that the ANN model produced more accurate predictions with lower errors compared to traditional methods [17].

3.0 METHODOLOGY

3.1 Data Collection

The rainfall data for this study were obtained from the Nigerian Meteorological Agency (NIMET) in Abuja. NIMET, a federal government agency, is tasked with advising the government on meteorological matters, including weather monitoring, climate forecasting, aviation weather support, and providing monthly and annual climate data to users in Nigeria. Monthly and annual rainfall data spanning three years (2019–2021) were filtered and processed for the study locations.

To collect climatic data, NIMET employs an Automatic Weather Observing Station (AWOS) system known as MIDAS IV AWOS. This automated weather station comprises a data logger, rechargeable battery, and meteorological sensors powered by solar panels or wind turbines, all mounted at an appropriate height on a mast. AWOS measures basic weather parameters such as air temperature, relative humidity, atmospheric pressure, precipitation, wind speed, wind direction, and solar radiation [18].

Additionally, NIMET uses rain gauges to ensure precise rainfall data collection. The rain gauge consists of a collection container placed in an open area, measuring precipitation in terms of the height of accumulated water in millimeters over a given period. Its upper section includes a cylindrical portion with a finely beveled brass rim, onto which a funnel is attached. This assembly fits securely atop an outer case with a splayed base. Inside the outer case is a cylindrical inner can, equipped with a brass-wire handle, containing a glass bottle with a narrow neck. The amount of rain collected is measured using specialized glass vessels known as rain measures.

3.2 Model Description

3.2.1 ITU-R rain attenuation model

The ITU-R P.618-13 model is widely recognized as an international standard for predicting the effects of rain on communication systems. This ITU-R model is derived from the rain attenuation model described by Dissanayake, Allnutt, and Haidara in [19], which has demonstrated superior performance in validation studies when compared to other models. The calculation of slant-path rain attenuation using point rainfall rate involves several parameters.

i. $R_{0.01}$: point rainfall rate for the location for 0.01% of an average year (mm/h)
ii. h_s: height above mean sea level of the earth station(km)
iii. θ: elevation angle (degrees)
iv. φ: latitude of the earth station (degrees)
v. f: frequency of operation (GHz)
vi. R_e: effective radius of the Earth (8500 km).
vii. Attenuation Coefficients: k and α

Figure 1(b) presents the slant path through rain and description of the parameters used in the corresponding step-by-step procedure for computational analysis.

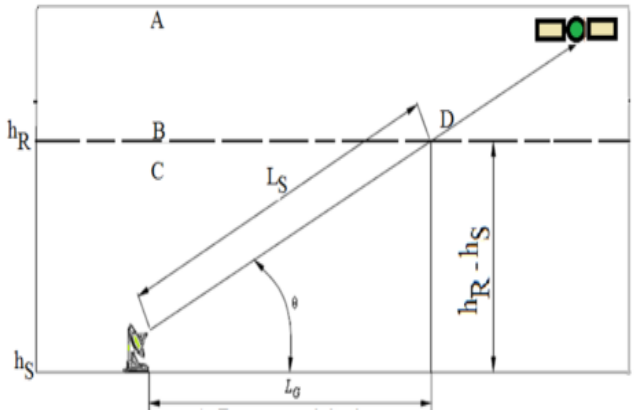

Figure 1(b): Slant Path through Rain

where,
A is frozen precipitation
B is Rain height
C is Liquid precipitation
D is Earth-Space path

Step 1: Determination the rain height, h_R, as given in Recommendation ITU-R P.839.

Step 2: Determination of the slant path length and the horizontal projection:

For $\theta \geq 5^o$

$$L_s = \frac{(h_R - h_s)}{sin\theta} \qquad 2$$

For $\theta < 5^o$

$$L_s = \frac{2(h_R - h_s)}{sin^2\theta + \frac{2(h_R - h_s)}{h_e}^{1/2} + sin\theta} \text{ km} \qquad 3$$

If $(h_R - h_s)$ is less than or equal to zero, the predicted rain attenuation for any time percentage is zero and the following steps are not required.

Step 3: Calculation of the horizontal projection, L_G, of the slant-path length from:

$$L_G = L_s Cos\theta \qquad \text{km} \qquad 4$$

Step 4: Determination of the rain rate at 0.01% for the location of interest over an average year, with an integration time of 1 min. However, if $R_{0.01}$ is equal to zero, the predicted rain attenuation is zero for any time percentage and the following steps are not required.

Step 5: Obtain the specific attenuation, γ_R, using the frequency-dependent coefficients and the rainfall rate, $R_{0.01}$. The relationship between rain rate R (mm/hr), and specific attenuation γ (dB/km) is given as:

$$\gamma_R = k(R_{0.01})^{\alpha} \qquad 5$$

Table 1 contains the values of k and α from ITU-R rain attenuation Model. Every frequency has its values of k and α which significantly plays role in specific attenuation.

Table 1: Frequency with associated values of k and α (ITU-R Model)

S/N	FREQUENCY	k	α
1	11GHz	0.0188	1.12
2	13GHz	0.023	1.13
3	14GHz	0.0255	1.14
4	15GHz	0.028	1.15
5	18GHz	0.030	1.16
6	23GHz	0.035	1.2

Calculating specific attenuations for the various frequencies for Rainfall rate ($R_{0.01}$) of 50mm/hr;

For 11GHz, specific attenuation is

$$\gamma_R = 0.0188 * (50)^{1,12}$$
$$= 1.503$$

For 13GHz;

$$\gamma_R = 0.023 * (50)^{1,13}$$
$$= 1.912$$

Table 2 is the calculated specific attenuations from various frequencies under considerations. It shows that as frequency increases, specific attenuation for various frequencies also increases.

Table 2: Frequencies with specific attenuations per kilometer distance

S/N	FREQ.	k	α	γ_R(dB/km)
1	11GHz	0.0188	1.12	1.5
2	13GHz	0.023	1.13	1.9
3	14GHz	0.0255	1.14	2.16
4	15GHz	0.028	1.15	2.52
5	18GHz	0.030	1.16	2.81
6	23GHz	0.035	1.2	3.83

Step 6: Calculation of the horizontal reduction factor, $r_{0.01}$, for 0.01% of the time:

$$r_{0.01} = \frac{1}{1+0.78\sqrt{\frac{L_G \gamma_R}{f} - 0.38(1-e^{-2L_G})}} \qquad 6$$

Step 7: Calculate the vertical adjustment factor, $V_{0.01}$, for 0.01% of the time:

$$\zeta = tan^{-1}\left(\frac{h_R - h_s}{L_G r_{0.01}}\right) \quad 7$$

$$\zeta > \theta, \quad L_R = \frac{L_G r_{0.01}}{Cos\theta} \text{ km}$$

else, $L_R = \frac{(h_R - h_s)}{Sin\theta}$ km

If $|\varphi| < 36$,

$$x = 36 - |\varphi| \text{ degrees} \quad 8$$

else, x = 0 degrees 9

$$r_{0.01} = \frac{1}{1+\sqrt{Sin\theta\left[31\left(1-e^{-\left(\frac{\theta}{1+x}\right)}\right)\frac{\sqrt{L_R \gamma_R}}{f^2} - 0.45\right]}} \quad 10$$

Step 8: The effective path length computation is as:

$$L_E = L_R v_{0.01} \text{ km} \quad 11$$

Step 9: Calculation of the attenuation exceeded for 0.01% of an average year

$$A_{0.01} = \gamma_R L_E \text{ dB} \quad 12$$

year, in the range 0.001% to 1%, done by the expression below:

If p 1% or $\geq |\varphi| \geq 36$: $\beta = 0$ 13

Step 10: Estimation of attenuation value exceeded for other percentages of an average

If p < 1 % and $|\varphi| < 36$ and $\theta \geq 25$

$$\beta = -0.005(|\varphi| - 36) \quad 14$$

Otherwise,

$$\beta = -0.005(|\varphi| - 36) + 1.8 - 4.25\ Sin\theta \quad 15$$

$$A_p = A_{0.01}\left(\frac{p}{0.01}\right)^{-(0.655+0.33\ln(p)-0.45\ln(A_{0.01})-\beta(1-p)\sin\theta)} \text{dB} \quad 16$$

In this case, Attenuation values exceeded for other percentages for various frequencies were calculated.

Fig. 2 illustrates that raindrops can cause Electromagnetic signals to be absorbed, scattered, diffracted, and depolarized.

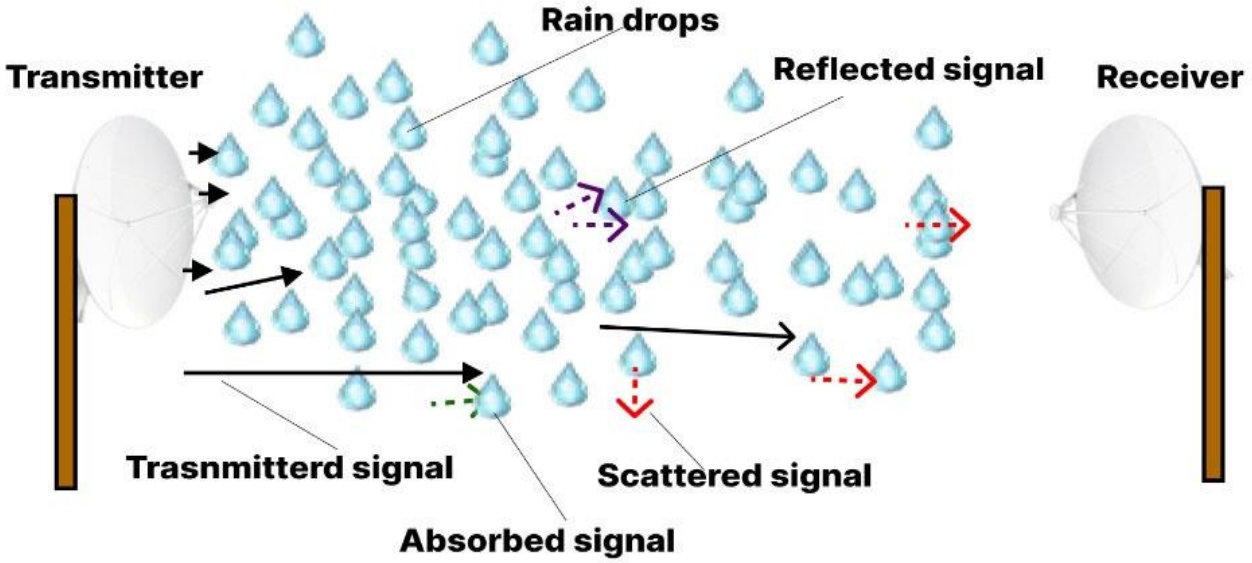

Fig.2.: Impact of Rain attenuations on microwave propagation

Table 3: Average rain fading rate of different frequency bands in City of Port Harcourt

S/N	Month	11G		13G		14G		15G		18G		23G	
		V	H	V	H	V	H	V	H	V	H	V	H
1	Jan	0.16	0.18	0.24	0.28	0.29	0.34	0.35	0.40	0.50	0.58	0.81	0.95
2	Feb	0.55	0.65	0.80	0.95	0.94	1.11	1.09	1.30	1.50	1.80	2.34	2.83
3	Mar	0.74	0.88	1.06	1.26	1.24	1.47	1.44	1.72	1.96	2.36	3.01	3.66
4	Apr	0.26	0.31	0.39	0.46	0.47	0.54	0.55	0.65	0.78	0.91	1.24	1.47
5	May	0.87	1.04	1.25	1.48	1.44	1.72	1.67	2.00	2.16	2.74	3.46	4.23
6	Jun	1.22	1.45	1.71	2.05	1.97	2.37	2.27	2.74	3.04	3.72	4.60	5.67
7	Jul	2.01	2.41	2.76	3.33	3.15	3.82	3.59	4.38	4.74	5.87	7.02	8.77
8	Aug.	0.97	1.16	1.36	1.65	1.60	1.91	1.85	2.22	2.49	3.03	3.80	4.66
9	Sep.	1.89	2.27	2.61	3.15	2.98	3.61	3.39	4.14	2.11	5.55	6.67	8.32

10	Oct	0.81	0.96	1.15	1.34	1.34	1.60	1.55	1.86	1.28	2.55	3.23	3.94
11	Nov.	0.46	0.54	0.67	0.80	0.79	0.93	0.93	1.10	0.99	1.53	2.01	2.41
12	Dec.	0.34	0.40	0.51	0.60	0.60	0.71	0.71	0.84	0.99	1.17	1.57	1.87

RESULTS

After an in-depth analysis of rain patterns and their corresponding effects on various frequency bands, the findings are presented here. This study examines how rain attenuation impacts signal propagation across multiple frequency ranges, highlighting the unique challenges posed to communication systems, particularly in Port Harcourt regions with high rainfall intensity. The results aim to provide valuable insights into the behavior of microwave signals under adverse weather conditions, such as rain-induced scattering and absorption. These findings offer practical data that can inform the design and optimization of communication systems, including satellite links and terrestrial microwave networks.

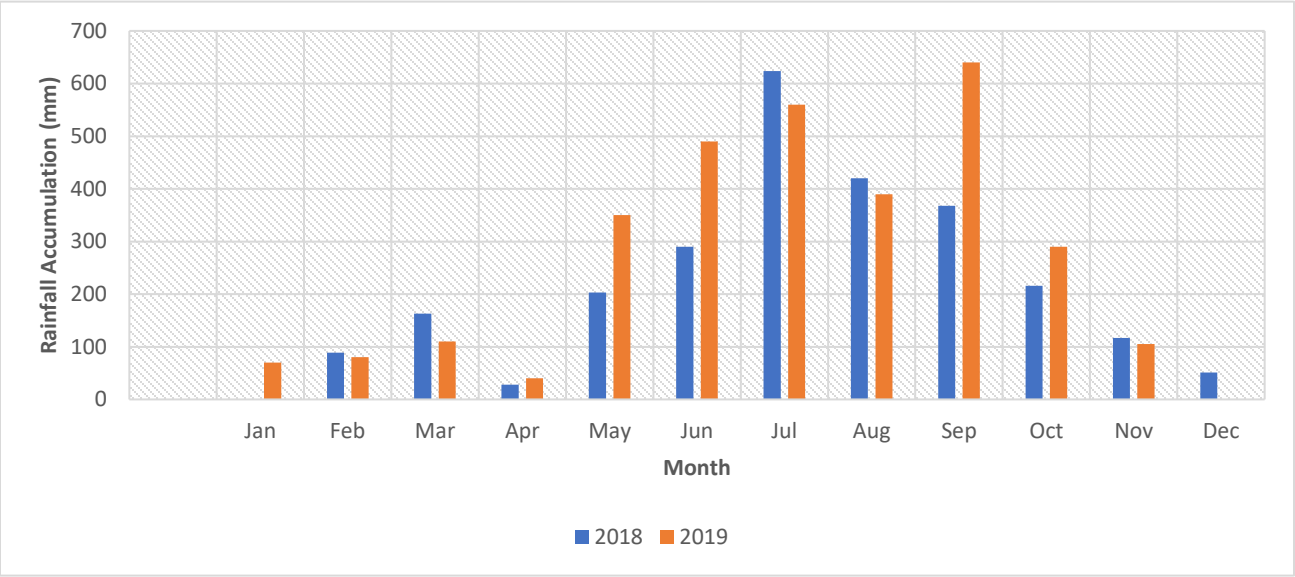

Fig.3: Average Rainfall analysis for the year 2018 and 2019 in city of Prot Harcourt

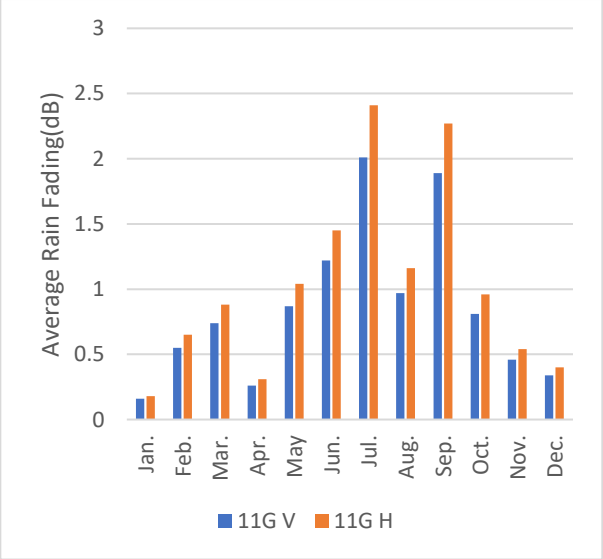

Fig.4: Average rain fading on Vertical and Horizontal Polarization for 11G Band for every month in one year

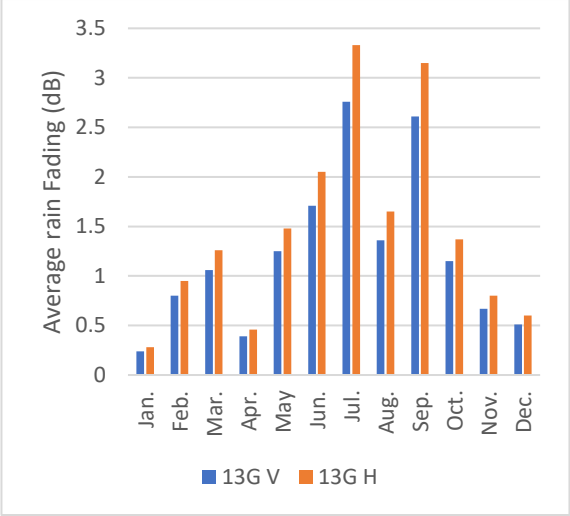

Fig. 5: Average rain fading on Vertical and Horizontal Polarization for 13G Band for every month in one year

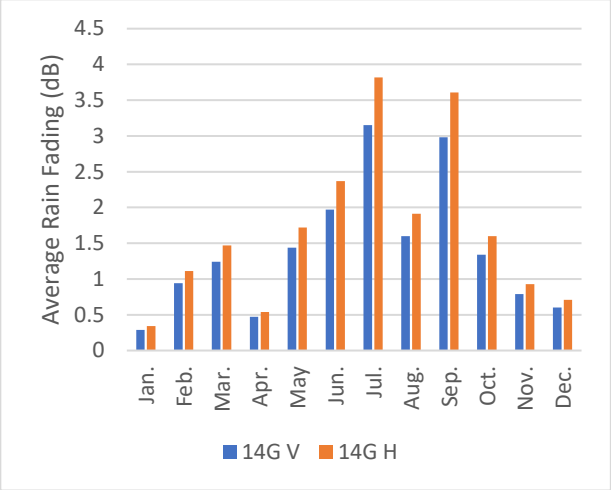

Fig. 6: Average rain fading on Vertical and Horizontal Polarization for 14G Band for every month in one year

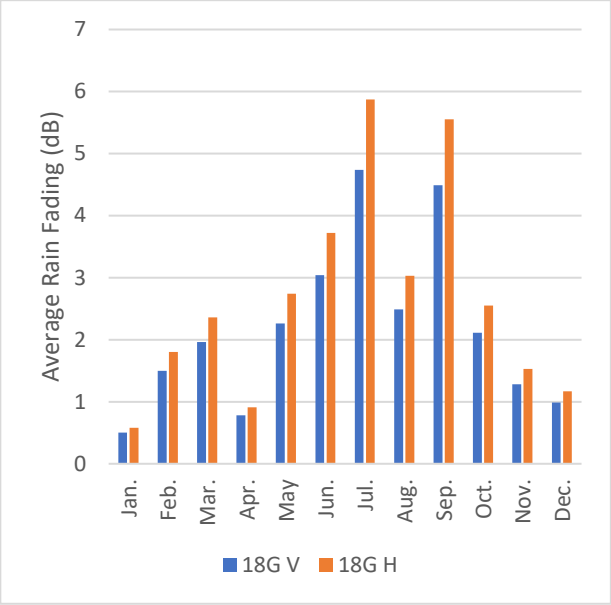

Fig. 7: Average rain fading on Vertical and Horizontal Polarization for 18G Band for every month in one year

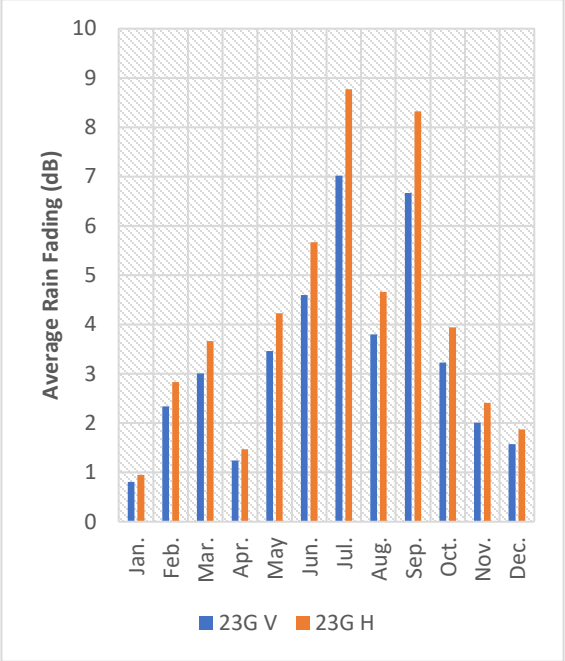

Fig. 8: Average rain fading on Vertical and Horizontal Polarization for 23G Band for every month in one year

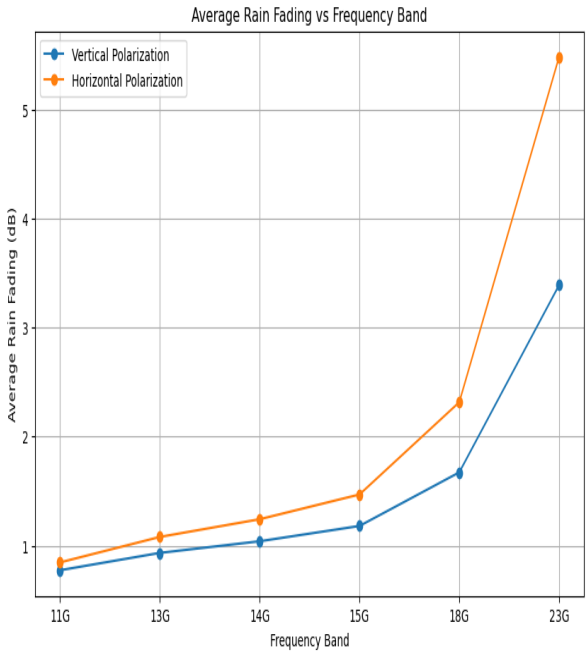

Fig. 9: Average rain fading increases as frequency increases as shown in both Vertical and Horizontal Polarization

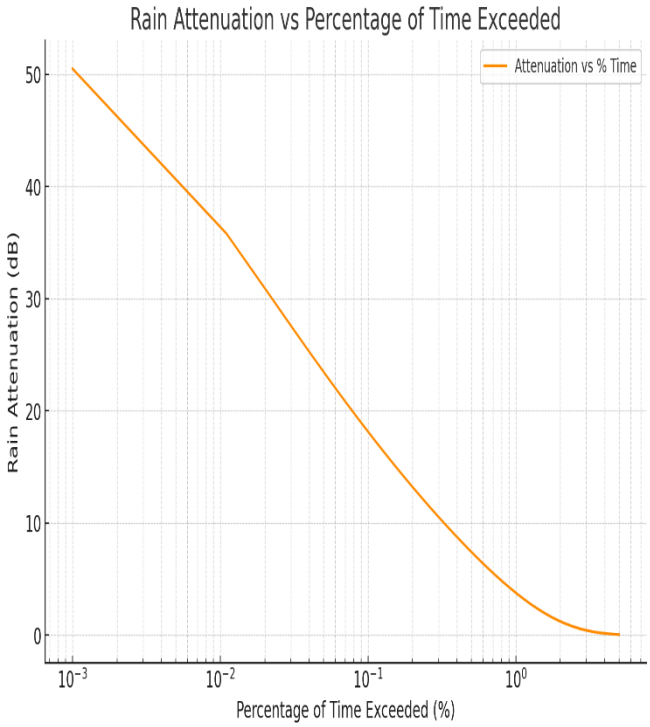

Fig. 10: Plot showing attenuation exceeded for different percentages of an average year

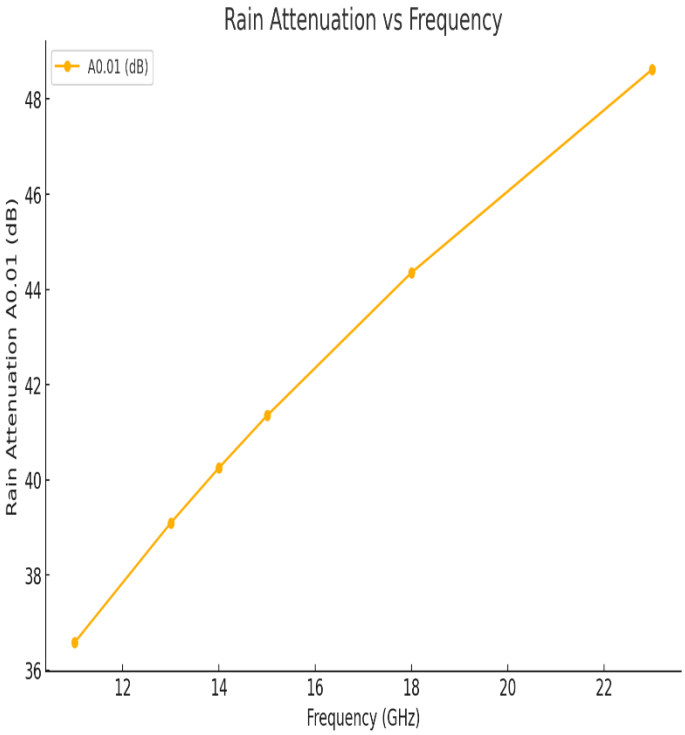

Fig.12: Simulated results for Rain Attenuation at different Frequencies

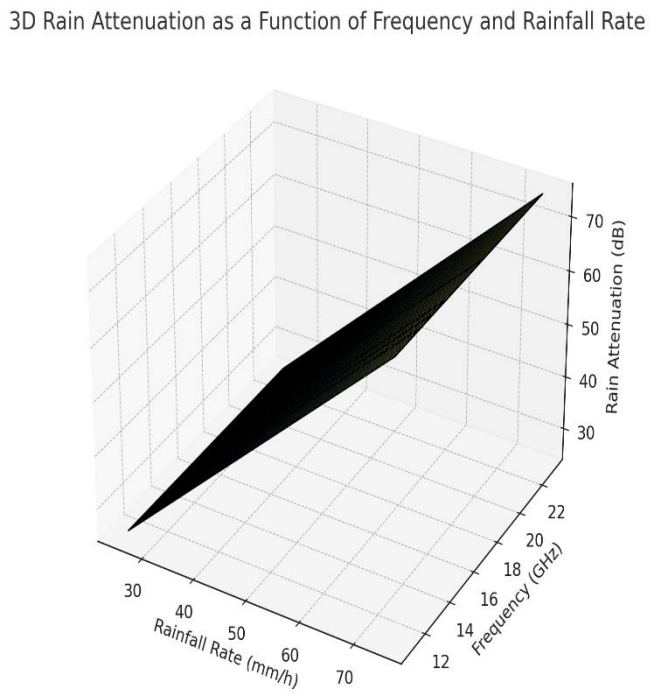

Fig. 11: 3D Plot Analysis of Predicted Rain Attenuation $A_{0.01}$ on different range of Frequencies and Rain Rate

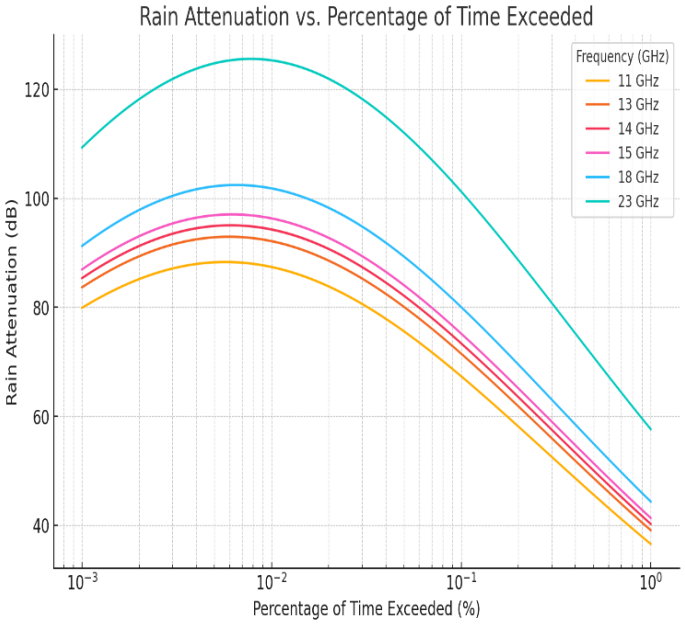

Fig. 13: Rain Attenuation for Percentage of Time Exceeded for various Frequencies

DISCUSSIONS

The results of this research provide a detailed reflection of the impact of rain attenuation on microwave propagation in the study area. Figure 3 presents a graphical analysis of two years of rainfall data from 2018 to 2019, showing rainfall accumulation in millimeters against the months. The data

reveals a gradual increase in rainfall starting in May, peaking in July for both years, and then gradually decreasing until December. Notably, September 2019 recorded the highest rainfall accumulation at 630 mm.

Fig. 4 through 8 display the plots of rain fading against months for both Vertical and Horizontal polarization. While the overall trends appear similar, distinct differences in rain fading are observed between the two polarizations each month. For instance, Fig. 4 shows that the average rain fading for Vertical polarization was 2 dB, whereas for Horizontal polarization, it was 2.4 dB, marking the highest rain fading for the 11 GHz band. This indicates that the month of July, with the highest rainfall accumulation, also experienced the most significant attenuation due to heavy rain.

Fig. 9 illustrates the relationship between average rain fading and frequency band, providing valuable insights into how rain fading varies with frequency. The results indicate that rain fading intensifies with increasing frequency. Additionally, Horizontal polarization exhibits a greater fading effect on microwave signals compared to Vertical polarization, as demonstrated in the simulated results in Figure 9.
Figure 10 is a simulated result of Rain attenuation A_p exceeded at other time percentages from 0.01% to 1%. Attenuation Exceeded for 0.01% of an Average Year $A_{0.01}$ was calculated, attenuation decreases as the percentage of time increases, demonstrating the relationship between the probability of rain attenuation and the magnitude of signal loss. For smaller percentages (0.01%), the attenuation is higher, reflecting severe conditions. As the percentage increases, attenuation decreases, corresponding to less extreme conditions.

Figure 11 is a 3D plot of Rain Attenuation as a function of Rainfall Rate and Frequency provides a comprehensive visualization of how these two variables influence attenuation on a microwave link. The X-axis represents the operating frequency of the microwave link, typically ranging from 11 GHz to 23 GHz in our case. Higher frequencies are more sensitive to rain-induced attenuation because they have shorter wavelengths, which are closer in size to raindrops. Y-axis indicates the intensity of rain in millimeters per hour. Rainfall rate is a critical factor because it directly impacts the density and size distribution of raindrops, which scatter and absorb microwave signals while Z-axis is the calculated attenuation value due to rain. It represents the loss in signal strength as a result of absorption and scattering of the electromagnetic waves by raindrops. As the frequency increases, the attenuation becomes more pronounced. At 11 GHz, attenuation is relatively modest even for high rainfall rates while at 23 GHz, the attenuation values are significantly higher due to stronger interaction between the shorter wavelength and the raindrops. Rain attenuation increases nonlinearly with rainfall rate. For light rain (25 mm/hr), the attenuation might be negligible for lower frequencies. However, for heavy rain (75 mm/hr), the attenuation grows rapidly.

The 3D plot shows how the combination of a high frequency and intense rainfall rate results in very high attenuation values. This highlights the need for careful planning in selecting operating frequencies, particularly in rain-prone regions. The plot helps to identify "safe zones" of operation combinations of frequency and rainfall rate where attenuation remains manageable for system performance.

In figure 12, each frequency (11 GHz, 13 GHz, 14 GHz, 15 GHz, 18 GHz) the results of the attenuation effect were obtained. As the frequency increases, rain attenuation $A_{0.01}$ also increases. This trend demonstrates that higher frequencies experience greater attenuation due to rain, making them more susceptible to signal degradation in rainy conditions. This model allows for predicting rain attenuation on microwave links at various frequencies, assisting in selecting optimal operational frequencies based on expected rain conditions in the area.
Figure 13 displays the relationship between rain attenuation and the percentage of time exceeded for different frequencies. Higher frequencies experience greater attenuation. As the frequency increases, the rain attenuation also increases significantly. At any given percentage, attenuation increases with frequency. At 0.001%, 23 GHz has the steepest curve due to its higher attenuation value of 57.63 dB. Lower frequencies have relatively flatter curves, representing reduced attenuation. The x-axis is on a logarithmic scale, covering a wide range of percentages (from 0.001% to 1%). This helps to clearly show the trend at very small percentages of time. Attenuation decreases rapidly as the percentage of time exceeds increases. At 0.001%, attenuation is very high, but for more frequent occurrences, it reduces substantially. The graph emphasizes the challenge of maintaining reliable microwave communication at higher frequencies, especially under heavy rain conditions.

CONCLUSION

This research highlights the significant impact of rain attenuation on microwave propagation in the study area, emphasizing the varying effects on Vertical and Horizontal polarization. The analysis of rain data from 2018 and 2019 demonstrates a seasonal pattern with peak rainfall in July, leading to the highest attenuation during that month. The findings reveal that Horizontal polarization experiences greater rain fading compared to Vertical polarization, with the severity of fading increasing with higher frequency bands.

Also, the simulated results from the ITU-R Model follows the same trends as the measured results obtained from analysis of data collected from Nigerian Metrological Agency (NIMET) which significantly highlighted the higher impacts of rain attenuation on higher frequency bands. The vulnerability of microwave links in this region calls for concern as totally attenuation occurs for minutes, hours and even days thereby grounding all communications that emanate from these links. This research underscores the importance of considering frequency range when designing and optimizing microwave communication systems in regions with substantial rainfall.

REFERENCE

1. Ulaganathen, K.; Rahman, T.B.A.; Islam, M.R.; Abdullah, K. (2020). Rain attenuation for 5G network in tropical region (Malaysia) for terrestrial link. *Prog. Electromagn. Res. Lett.*, **90**, 99–104. https://doi.org/10.1109/MICC.2017.8311727.
2. Ekpe, U.M.; Umoh, V.B.; Agbeb, N.S. (2021). Eliminating the digital divide in Nigeria: Policy direction and 5G deployment methodology. In *Proceedings of the 2021 1st International Conference on Multidisciplinary Engineering and Applied Science (IC-MEAS)*, Abuja, Nigeria, 15–16 July 2021. https://doi.org/10.1109/ICMEAS52683.2021.9692399.
3. Sowande, O.; Idachaba, F.; Ekpo, S.; Faruk, N.; Uko, M.; Ogunmodimu, O. (2022). Sub-6 GHz, 5G spectrum for satellite-cellular convergence broadband internet access in Nigeria. *Int. Rev. Aerosp. Eng.*, **15**(2). https://doi.org/10.15866/irease.v15i2.20240.
4. Huang, J.; Cao, Y.; Raimundo, X.; Cheema, A.; Salous, S. (2019). Rain statistics investigation and rain attenuation modeling for millimeter wave short-range fixed links. *IEEE Access*, **7**, 156110–156120. https://doi.org/10.1109/ACCESS.2019.2949437.
5. Isabona, J.; Kehinde, R.; Imoize, A.L.; Ojo, S.; Faruk, N. (2022). Large-scale signal attenuation and shadow fading measurement and modeling for efficient wireless network design and management. In *Proceedings of the 2022 IEEE Nigeria 4th International Conference on Disruptive Technologies for Sustainable Development (NIGERCON)*, Lagos, Nigeria, 5–7 April 2022, pp. 1–5.
6. Isabona, J.; Imoize, A.L.; Rawat, P.; Jamal, S.S.; Pant, B.; Ojo, S.; Hinga, S.K. (2022). Realistic prognostic modeling of specific attenuation due to rain at microwave frequency for tropical climate region. *Wireless Communication and Mobile Computing*, **2022**, 8209256. https://doi.org/10.1155/2022/8209256.
7. Ogbonna, D.N.; Amangabara, G.T.; Ekere, T.O. (2007). Urban solid waste generation in Port Harcourt Metropolis and its implications for waste management. *Management of Environmental Quality: An International Journal*, **18**(1).
8. Oyegun, C.U. (1999). Geology of Port Harcourt. In Oyegun, C.U., and Adeyemo, A. (Eds.), *Port Harcourt Region*. Paragraphics, Port Harcourt.
9. Obiyemi, O.O.; Ojo, J.S.; Ibiyemi, T.S. (2014). Performance analysis of rain rate models for microwave propagation designs over tropical climate. *Prog. Electromagn. Res. M*, **39**, 115–122. https://doi.org/10.2528/PIERM14083003.
10. Budalal, A.A.; Shayea, I.; Islam, M.R.; Azmi, M.H.; Mohamad, H.; Saad, S.A.; Daradkeh, Y.I. (2022). Millimeter-wave propagation channel based on NYUSIM channel model with consideration of rain fade in tropical climates. *IEEE Access*, **10**, 1990–2005. https://doi.org/10.1109/ACCESS.2021.3135382.
11. Seah, S.J.; Jong, S.L.; Lam, H.Y.; Din, J. (2022). Rain fade margin of terrestrial line-of-sight (LOS) links for 5G networks in Peninsular Malaysia. *Int. J. Microwave Wireless Technol.*, **14**, 750–760. https://doi.org/10.1017/S1759078721000751.
12. Han, C.; Bi, Y.; Duan, S.; Lu, G. (2019). Rain rate retrieval test from 25-GHz, 28-Hz, and 38-GHz millimeter-wave link measurement in Beijing. *IEEE J. Sel. Top. Appl. Earth Obs. Remote Sens.*, **12**, 2835–2847. https://doi.org/10.1109/JSTARS.2019.2918507.
13. Nabangala, M.; Africa, S. (2018). Rainfall attenuation prediction model for dynamic rain fade mitigation technique considering millimeter-wave communication. *ResearchSpace*. Available online: https://researchspace.ukzn.ac.za/xmlui/handle/10413/17179 (accessed on 15 September 2022).
14. Olurotimi, E.O. (2021). Estimation of cloud attenuation over some coastal cities for satellite space links in South Africa. *J. Phys. Conf. Ser.*, **1874**, 12011. https://doi.org/10.1088/1742-6596/1874/1/012011.
15. Ferdowsi, A.; Whitefield, D. (2021). Deep learning for rain fade prediction in satellite communications. In *Proceedings of the 2021 IEEE GLOBECOM Workshops (GC Workshops)*, Madrid, Spain, 7–11 December 2021, pp. 1–6. https://doi.org/10.1109/GCWkshps52748.2021.9682090.
16. Kamoru, K.; Kolawole, K.K.; Mayowa, O.; Theophilus, E. (2021). Development of rain attenuation prediction in southwest Nigeria on terrestrial link using artificial neural networks. *Int. J. Commun. Inf. Technol.*, **2**, 33–39. Available online: https://www.computterscience-journals.com/ijcit/article/31/3-1-1-298.pdf (accessed on 5 August 2022).
17. Islam, M.A.; Maiti, M.; Ghosh, P.K.; Sanyal, J. (2021). Machine learning-based rain attenuation prediction model. *Lect. Notes Netw. Syst.*, **147**, 15–22. https://doi.org/10.1007/978-981-15-8366-7_3.
18. Aderinto, S. (2018). The new automated meteorological observation at four major airports in Nigeria. *Meteorological Data and Calculations*, pp. 1–14.
19. Dissanayake, A.; Allnutt, J.; Haidara, F. (1997). A prediction model that combines rain attenuation and other propagation impairments along earth-satellite paths. *IEEE Trans. Antennas Propag.*, **45**(10), 1546–1558.